Int. J. Electrochem. Sci., 7 **(2012)** 4302 - 4313

International Journal of
ELECTROCHEMICAL
SCIENCE
www.electrochemsci.org

Fabrication of Prussian Blue/Multi-Walled Carbon Nanotubes Modified Glassy Carbon Electrode for Electrochemical Detection of Hydrogen Peroxide.

Abdullahi Mohamed Farah[1], *Ntaote David Shooto*[1], *Force Tefo Thema*[1], *Johannes Sekomeng Modise*[2] *and Ezekiel Dixon Dikio*[1,*]

[1] Department of Chemistry, Vaal University of Technology, P. O. Box X021,Vanderbijlpark 1900, Republic of South Africa.
[2] Institute of Chemical and Biotechnology, Vaal University of Technology, P. O. Box X021, Vanderbijlpark 1900, South Africa.
[*]E-mail: ezekield@vut.ac.za

Received: 4 March 2012 / *Accepted:* 31 March 2012 / *Published:* 1 May 2012

Prussian blue nanoparticles synthesized from $K_4[Fe(CN)_6]3H_2O$ and $Fe(NO_3)_3.9H_2O$, were characterized by Fourier transform infrared (FT-IR), X-ray diffraction (XRD), Energy dispersive spectroscopy (EDS), Scanning electron microscopy (SEM), and Raman spectroscopy. Prussian blue nanoparticles were modified on a glassy carbon electrode as a mediator of carbon nanotube; three electrodes GC-Bare, GC-PB and GC-CNT-PB were fabricated. Cyclic voltammetry were employed to characterize electrodes at pH ranges of (3 - 7.4) in 0.1M phosphate buffer solution, in the absence or presence of 25 μM of H_2O_2. Compared with Prussian blue (PB) modified on glassy carbon electrode (GC-PB), the GC-CNT-PB electrode exhibits much electrochemical stability, much wider pH range and high response currents for the reduction of hydrogen peroxide (H_2O_2).

Keywords: Prussian blue, electrochemical, carbon nanotubes, Hydrogen peroxide

1. INTRODUCTION

In the last two decades, coating of electrode surfaces with various electroactive materials is an interesting area of research in designing electrochemical sensors. Several organic and inorganic modifiers have been employed in conducting substrate electrodes to make chemically modified electrodes [1-2]. These modifiers include tungsten oxide (WO_3) and Prussian blue (PB) [3]. Prussian blue is an inorganic polycrystalline substance which has been extensively investigated due to its electrochemical, photophysical, electrochromic and magnetic properties and potential analytical

applications [4-6]. In 1978, Neff *et al* [7] reported for the first time the successful deposition of Prussian blue on a platinum foil as well as its electrochemical behavior [8-10]. A large number of studies followed, and different methods for the preparation of PB-modified electrodes have been described [11]. Prussian blue has been modified for many electrodes such as gold electrode [12], graphite electrode [5], edge plane pyrolytic graphite electrode [13] and glassy carbon electrode [14]. Prussian blue nanoparticles can be easily synthesized by the addition of aqueous solution of iron(III) ions to an aqueous ferrocyanide solution under vigorous stirring at room temperature [15-16]. These nanoparticles make two structural forms (soluble $KFe^{III}[Fe^{II}(CN)_6]$ and insoluble $(Fe_4^{III}[Fe^{II}(CN)_6]_3$ Prussian blue).

The two forms have similar structure, but have different extents of peptization with potassium ions. Replacement of potassium ions with ferric ions in a soluble PB would produce insoluble PB [17-18].Since the discovery of carbon nanotubes (CNTs) by lijima in 1991 [19], research on CNTs have improved speedily and have become one of the most attractive parts of nanotechnology in the world [20-21]. These nanotubes are known to possess interesting chemical and physical properties such as electric conductivity, chemical stability, mechanical and tensile strength [22-23]. The importance of these unique properties can be improved or fine-tuned towards specific purposes by chemical modification [24], therefore, the combination of PB and CNTs has received research interest. CNTs are considered to be good mediator for PB-modified electrodes due to their good electric conductivity and the property of being particle carriers [25-26]. Electrodes modified with different electroactive materials have the ability to detect hydrogen peroxide, H_2O_2, at low potentials. On the other hand, hydrogen peroxide, H_2O_2, is an essential mediator in many fields such as food, pharmaceutical, clinical diagnostic environmental protection and in industries [27-28]. Since its discovery almost two decades ago, Prussian blue or ferric ferrocyanide, electrodeposited onto an electrode surface, could act as an electrocatalyst for hydrogen peroxide reduction [29]. Although accurate determination of hydrogen peroxide (H_2O_2) is of great importance. In this study, PB deposited on multi-walled carbon nanotubes (MWCNTs) modified glassy carbon electrode (GCE) has been used in the electrochemical determination of hydrogen peroxide.

2. EXPERIMENTAL

2.1. Reagents and apparatus

Glassy carbon electrodes (GCE) were purchased from BAS Inc (Tokyo Jaban), and Multi-walled carbon nanotubes (MWCNT) were obtained from our research group Ndwandwe *et al.*[30]. Sodium dihydrogen phosphate (NaH_2PO_4), disodium hydrogen phosphate (Na_2HPO_4), potassium hexacyanoferrate ($K_4[Fe(CN)_6]3H_2O$, iron nitrate nonahydrate ($Fe(NO_3)_3.9H_2O$ and aluminium oxide (Al_2O_3) were purchased from Sigma-Aldrich. Acetone (C_3H_6O), *N*,*N*-dimethylformamide (DMF), hydrogen peroxide (H_2O_2) nitric acid (HNO_3), hydrochloric acid (HCl) were also obtained from Sigma–Aldrich. All chemicals were of analytical grade and used as received without further purification.

2.2. Electrochemical measurements

Electrochemical measurements were performed using an auto-lab potentiostat (663 VA stand metrohm Swiss mode). A convectional three-electrode system was employed, Ag/AgCl (3M KCl) as reference electrode, platinum electrode as a counter electrode and glassy carbon electrode (GC) modified with multi-walled carbon nanotubes (MWCNT) and Prussian blue (PB) as working electrode in all experiments. A 0.1M phosphate buffer solution (PBS) with different pH solutions was used as electrolyte solution.

2.3. Synthesis of Prussian blue nanoparticle

Prussian blue nanoparticles were synthesized as follows: An aqueous solution of $Fe(NO_3)_3.9H_2O$ was added to an aqueous solution of same equal molar mass of $K_4[Fe(CN)_6]3H_2O$. The reaction mixture was vigorously stirred for 10 min. Dark blue precipitate obtained were centrifuged, washed with distilled water three times and with methanol once , and then dried in an oven at 80^{o}C to yield insoluble Prussian blue nanoparticles [31].

2.4. Preparation of modified electrodes

The GCE surfaces (3 mm in diameter) were cleaned by gentle polishing in aqueous slurry of alumina on a mesh paper. The electrode was then subjected to ultrasonic vibration in acetone to remove residual alumina particles that might be trapped at the surface of the electrode, and then subjected to ultrasonic vibration in deionized water before drying. GC-MWCNTs was prepared with 50 mg of MWCNTs was dispersed in 5 ml of *N*,*N*-dimethylformamide (DMF) with the aid of ultrasonic mixing for 30 min to form a stable black suspension. About 20 μL drop of MWCNTs/DMF solution were dropped on bare GC electrode and dried in an oven at 50^{o}C for 5 min. The modified electrode is herein designated as GC-MWCNTs. The PB film was prepared by sequential deposition method as described by Han *et al* [32]. GC-Bare or GC-MWCNTs electrodes were immersed in $Fe(NO_3)_3.9H_2O$ solution for 30min, with stirring after which the electrodes were rinsed, dried and then immersed in $K_4[Fe(CN)_6].3H_2O$ solution and stirred for another 30 min, followed by a re-rinsing and a re-drying processes to complete the deposition cycle. The electrode obtained thereafter, were described as GC-PB and GC-MWCNTs-PB respectively.

2.5. Characterization

The morphological features of Prussian blue nanoparticles were analyzed by Raman spectroscopy, FE-SEM, EDS, and XRD. The Raman spectra were obtained by a Raman spectroscope, Jobin-Yvon HR800 UV-VIS-NIR Raman spectrometer equipped with an Olympus BX 40 attachment. The excitation wavelength was 514.5 nm with an energy setting of 1.2 mV from a coherent Innova model 308 argon-ion laser. The Raman spectra were collected by means of back scattering geometry

with an acquisition time of 50 seconds. The surface morphology and EDS measurements were recorded with a JEOL 7500F Field Emission scanning electron microscope. Powder X-ray diffraction (PXRD) patterns were collected with a Bruker AXS D8 Advanced diffractometer operated at 45 kV and 40 mA with monochromated copper Kα1 radiation of wavelength (λ = 1.540598) and Kα2 radiation of wavelength (λ = 1.544426). Scan speed of 1 s/step and a step size of 0.03°.

3. RESULTS AND DISCUSSION

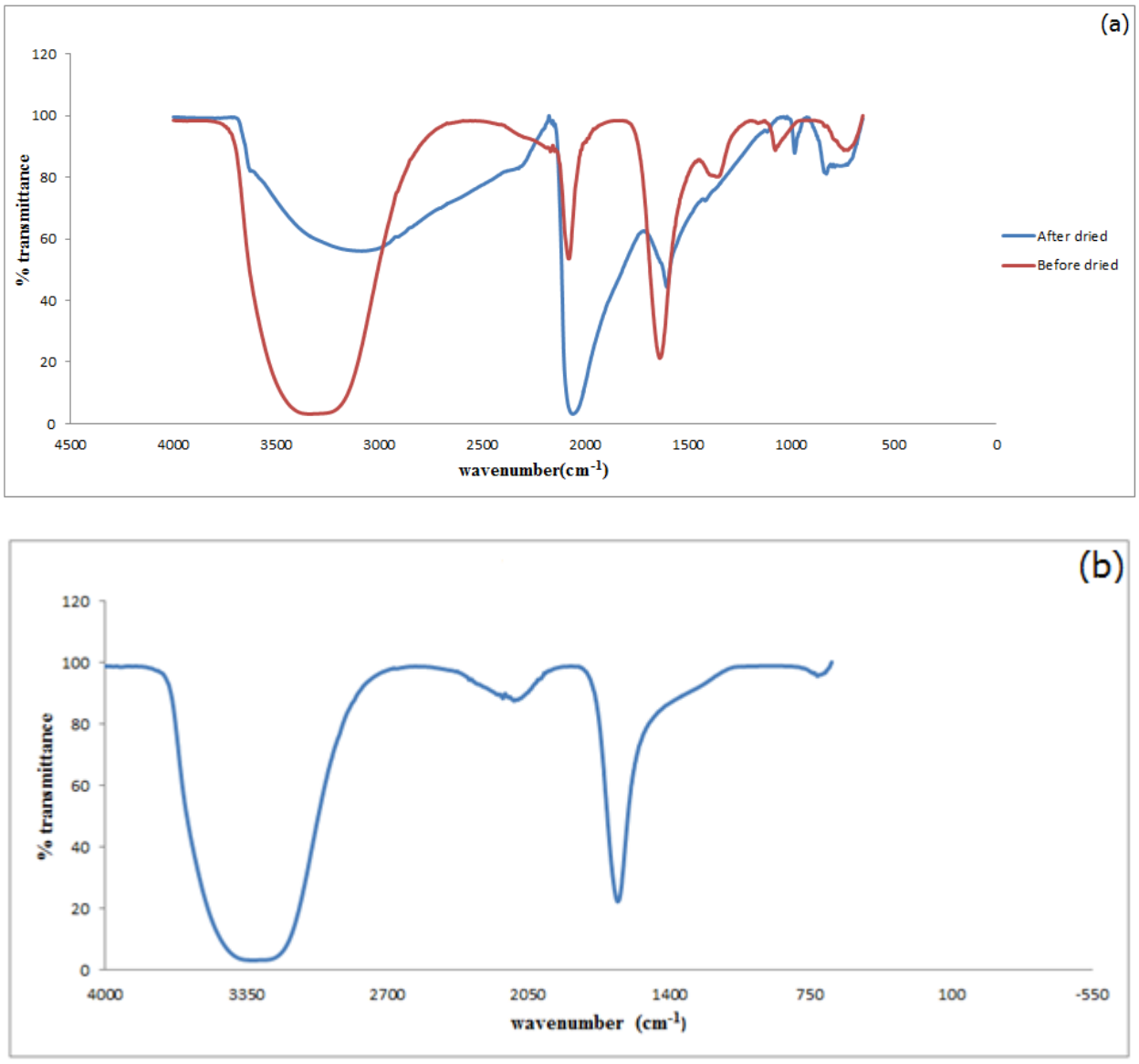

Figure 1. Fourier Transform infrared (FTIR) spectra of (a) Prussian blue, before and after drying and (b) composite Prussian blue with multiwall carbon nanotube.

The Fourier transform infrared spectra of synthesized Prussian blue nanoparticles before and after drying and that of a composite formed between Prussian blue and multiwall carbon nanotube are

presented in figure 1. FT-IR spectra were measured in the range of 4000.0 – 650.0 cm^{-1}. The spectrum of Prussian blue before drying, figure 1(a), shows a strong broad band at 3336 cm^{-1} which is assigned to the stretching modes of O–H group and H–O–H bending mode of water. This band shows that water molecules in the Prussian blue is coordinated in the shell of high spin iron or occupying interstitial positions as uncoordinated water. The sharp peak at 2077cm^{-1} is a characteristic peak of Fe-CN bond and is linked to the stretching vibration of Fe-CN. The strong peak at 2057 cm^{-1} is a characteristic vibrational peak of PB which is attributed to the stretching vibration of the CN group. The FTIR of dried PB nanoparticle show a reduced broad band at 3325 cm^{-1} indicating the removal of water. The spectra of the PB/MWCNT composite, figure 1(b), show a broad band centered around 3350 cm^{-1} and a new sharp band at 1637 cm^{-1}. These two bands are due to the presence of OH and CN groups in the nanocomposite. The presence of these two bands further demonstrates the formation of the composite. The X-ray diffraction (XRD) spectrum of Prussian blue nanoparticle is presented in figure 2.

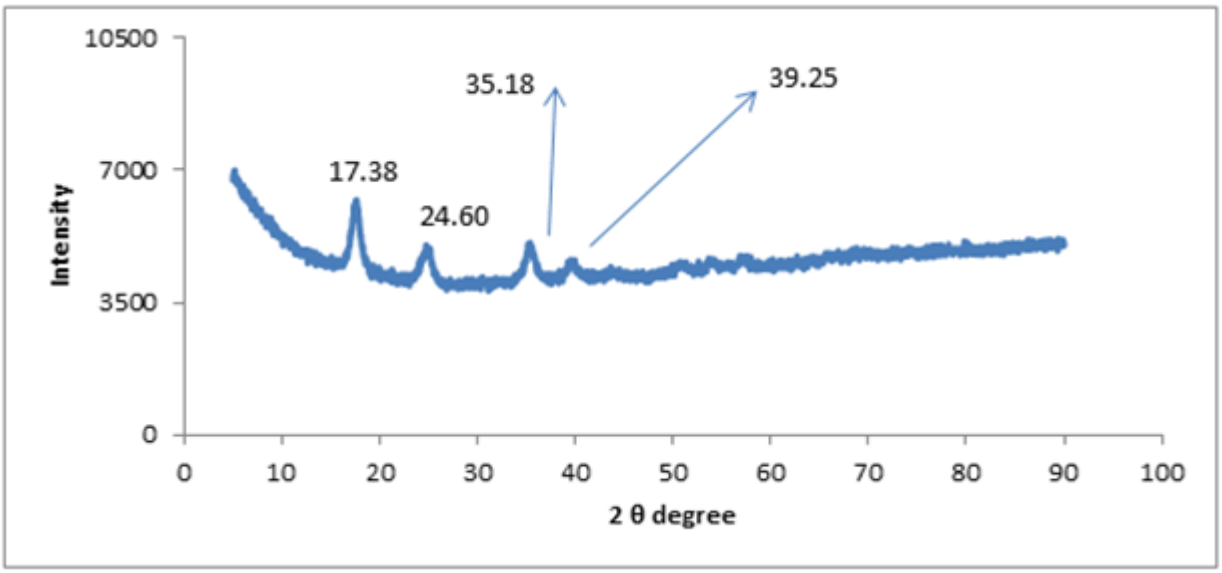

Figure 2. X-ray Diffraction (XRD) spectra of Prussian blue nanoparticles

X-ray diffraction discovers the geometry or shape of a molecule using x-ray diffraction technique which is based on the elastic scattering of x-rays from structures that have long range order. The spectra show a diffraction peaks at 17.380, 24.600, 35.180 and 39.250 which can be allocated to the Prussian blue phase (200, 220, 222, and 400) crystal planes respectively. These peaks can be related to face-centered cubic structure of PB with space group Fm3m. The energy dispersive spectroscopy (EDS) spectrum of Prussian blue nanoparticle is presented in figure 3. Energy dispersive x-ray spectroscopy (EDS) is an analytical technique used for the elemental analysis or chemical characterization of a sample. The EDS spectra of synthesized Prussian blue nanoparticles indicate the presence of the elements carbon, oxygen, potassium, iron and chlorine employed during synthesis. This confirms the successful synthesis of Prussian blue. The scanning electron micrograph (SEM)

image of Prussian blue nanoparticles is presented in figure 4. The SEM was used to determine the particle size and distribution of the as-synthesized Prussian blue nanoparticles.

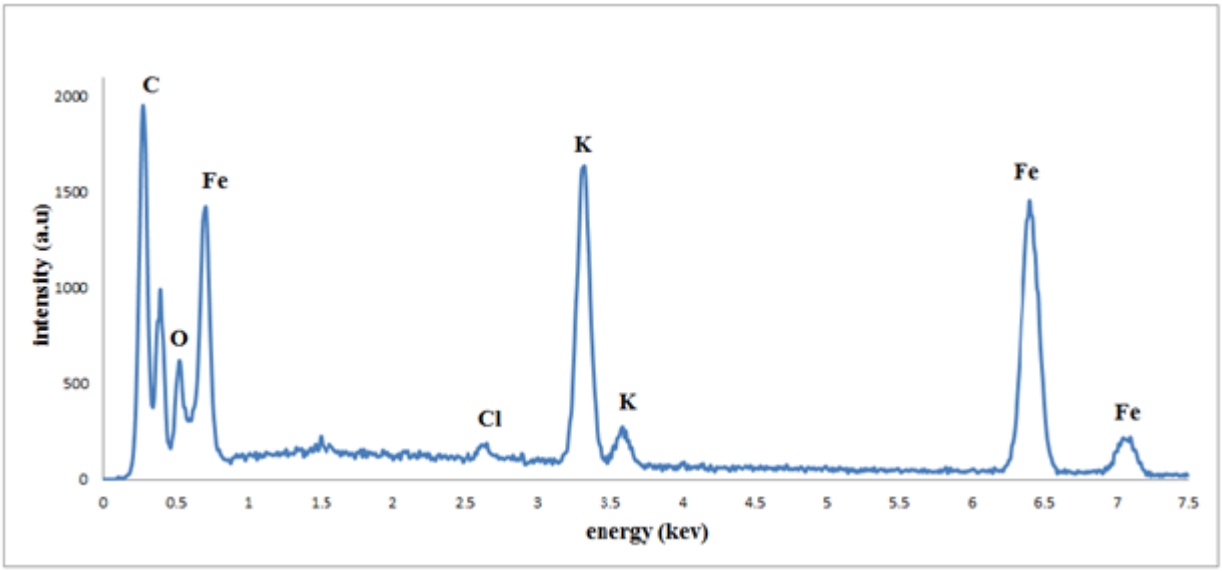

Figure 3. Energy Dispersive Spectroscopy (EDS) of Prussian blue nanoparticles

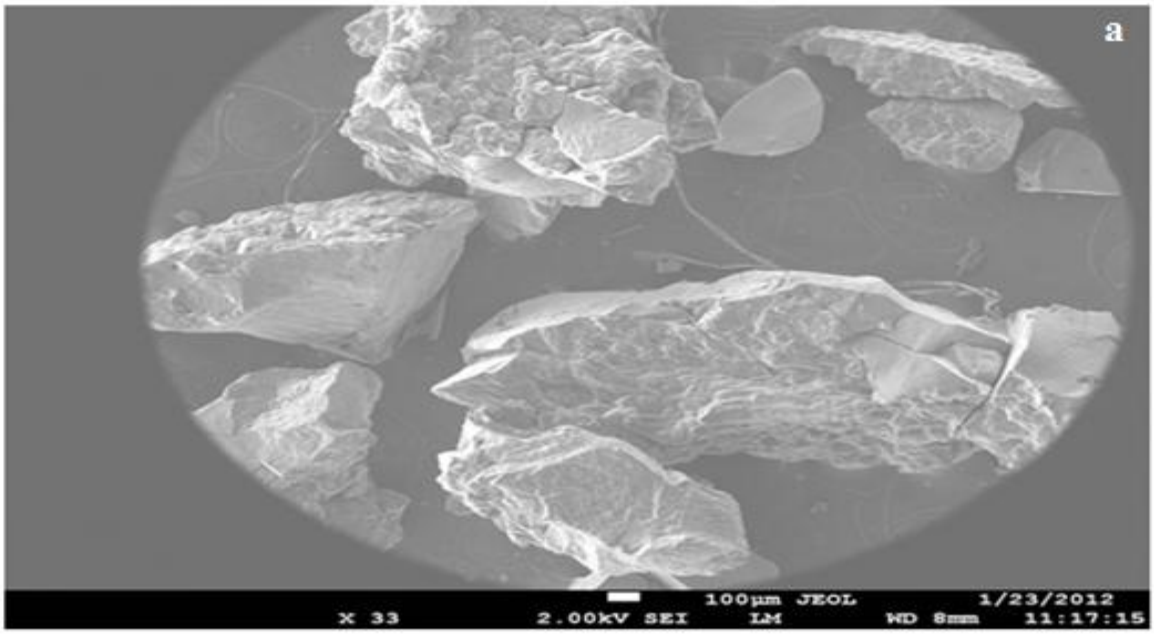

Figure 4. Scanning Electron Micrograph (SEM) of Prussian blue nanoparticles

The SEM image at 100 µm, show the PB as aggregates of nanoparticles of high dimension with no precise shape. The Raman spectra of Prussian blue nanoparticles are presented in figure 5.The Raman spectra of Prussian have shown that there is a strong vibrational band at 2154.96cm-1 which is caused by the stretching vibration of carbon nitrogen triple bond group of Prussian blue. Where the

other peaks at 1254.35, 507.47 and 275.49cm^{-1} are expected to have relation to the presence of co-precipitated ferricyanide ion.

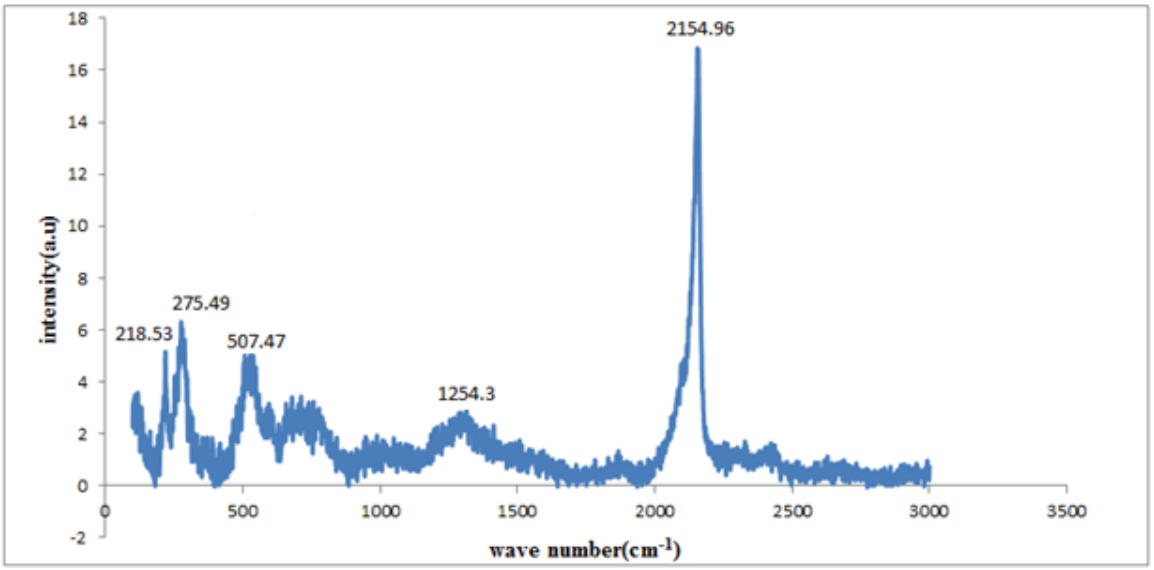

Figure 5. Raman Spectra of Prussian blue nanoparticles

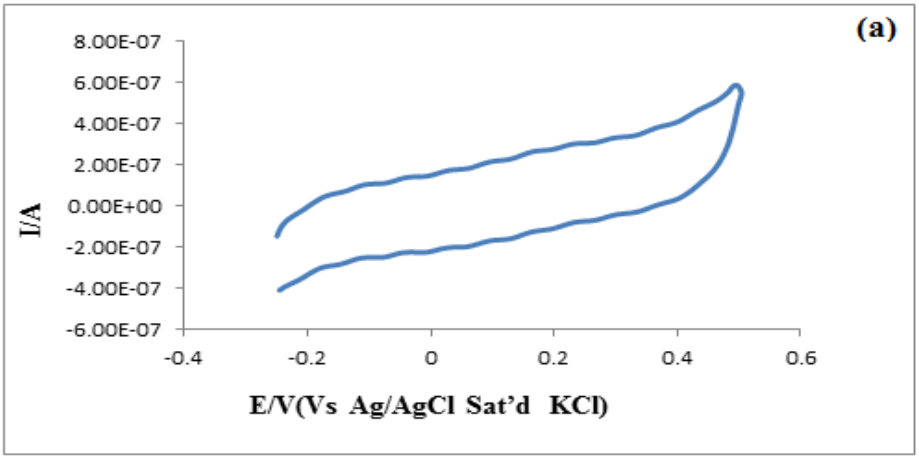

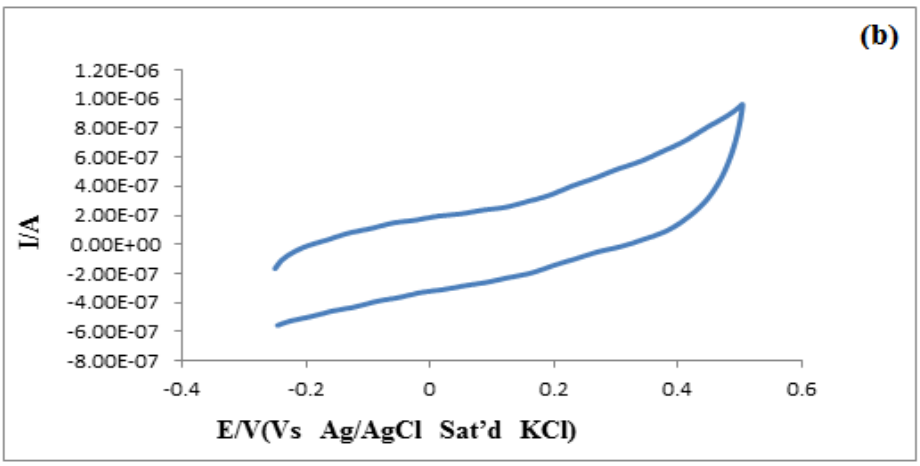

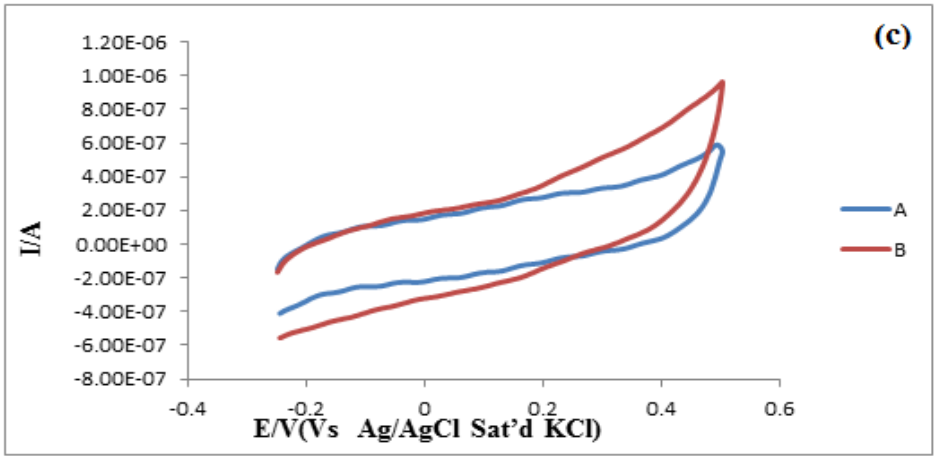

Figure 6. Cyclic voltammograms of bare-GC electrode (a) before and (b) after injection of 25µl H_2O_2 in 0.1M PBS pH 7.4 (c) overlay of the two voltammograms.

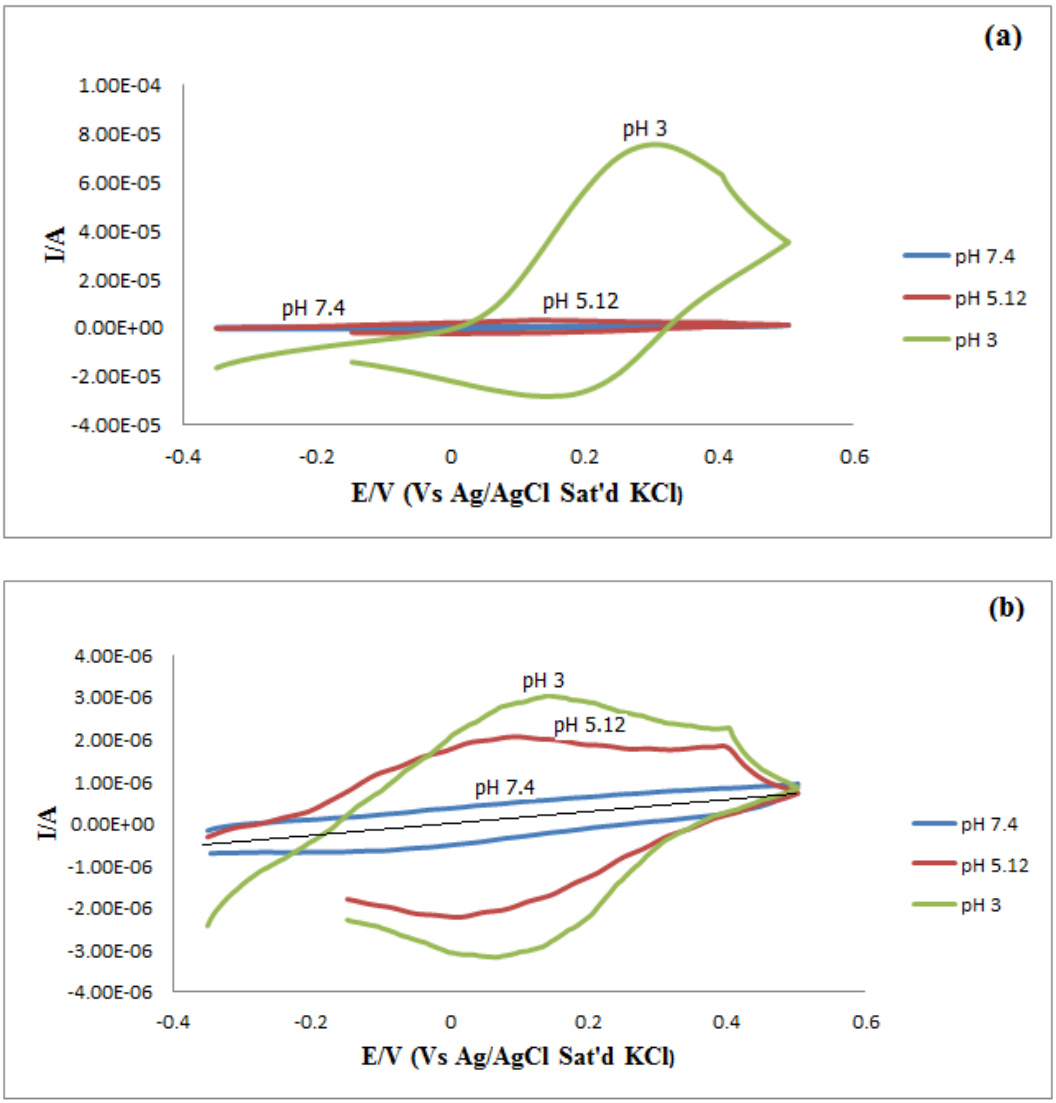

Figure 7. Cyclic voltammograms of GC-PB electrode (a) before and (b) after injection of 25µl H_2O_2 in 0.1M PBS at different pH values**.**

The electrochemical properties of bare GC, GC-PB and GC-MWCNT-PB electrodes were studied in 0.1 M phosphate buffer solution at different pH values and at a scan rate of 100 mV/s. The cyclic voltammograms of bare GC electrode in the presence and absence of hydrogen peroxide in 0.1 M phosphate buffer solution pH 7.4 is presented in figure 6 (a and b). The overlay of the electrode response in the presence and absence of hydrogen peroxide is presented in figure 6(c). As can be seen, a small anodic response is observed. The bare GC electrode does not have the ability to detect hydrogen peroxide.

The cyclic voltammogram of GC-PB electrode in the presence and absence of hydrogen peroxide in 0.1 M phosphate buffer solution at pH 3, pH 5.12 and pH 7.4 are presented in figure 7. The GC-PB electrode in the absence of hydrogen peroxide, figure 7(a) does not show any electrochemical response at pH 5.12 and pH 7.4, while at pH 3, anodic and cathodic responses are observed. In the presence of hydrogen peroxide, figure 7(b), responses are observed at pH 7.4, pH 5.12 and pH 3. The highest response is observed at pH 3 and the lowest response is observed at pH 7.4. The high response at pH 3 is due to the fact that at high pH, Prussian blue losses its stability. Hydrogen peroxide also affects the response of the modified electrode significantly at pH 7.4 and pH 5.12. The cathodic responses are greater than the anodic responses at all pH values. The anodic response at pH 3 for the electrode in the absence of hydrogen peroxide, is also greater than the anodic response in the presence of hydrogen peroxide. On the other hand, the cathodic responses at all pH values in the presence of hydrogen peroxide are greater than the cathodic responses in the absence of hydrogen peroxide.

The cyclic voltammograms of GC-MWCNT-PB electrode in the presence and absence of hydrogen peroxide in 0.1 M phosphate buffer solution at pH 3, pH 5.12 and pH 7.4 are presented in figure 8. In the absence of hydrogen peroxide, figure 8(a), electrochemical responses are observed at pH 5.12 and 7.4 with a very negligible response observed at pH 3. The anodic response at pH 5.12 and 7.4 are very significant with the peak at pH 5.12 higher than at pH 7.4. The cathodic responses at pH 5.12 and 7.4 are also significant but less than the anodic response.

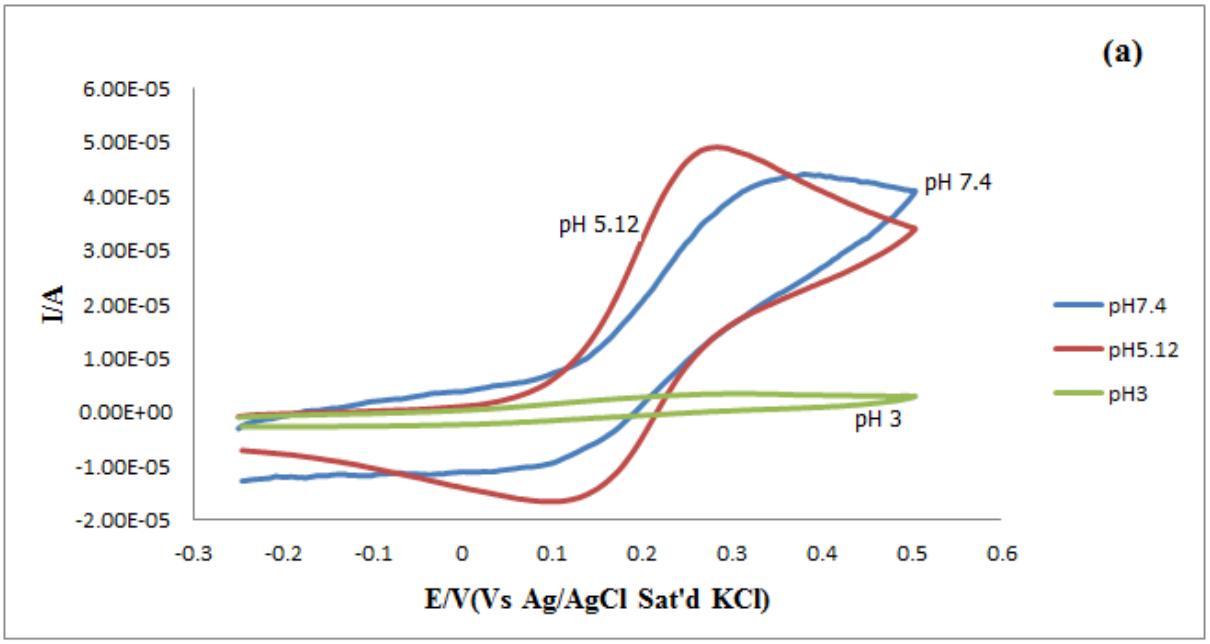

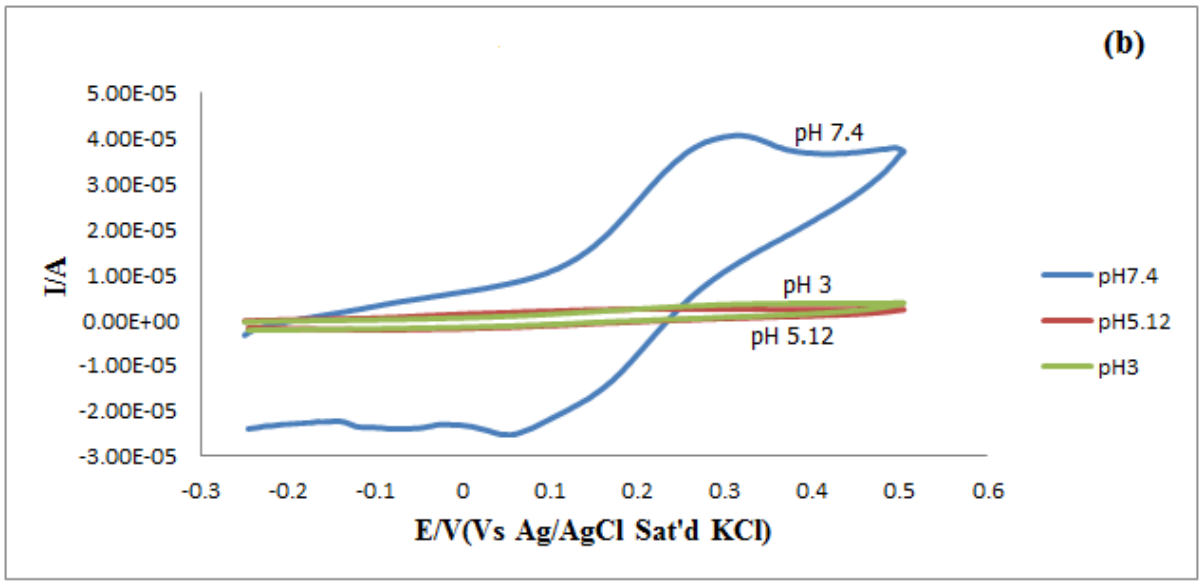

Figure 8. Cyclic voltammograms of GC-MWCNT-PB electrode (a) before and (b) after injection of 25µl H_2O_2 in 0.1M PBS with different pH values.

Again, at pH 5.12, a higher cathodic response is observed than at pH 7.4. In the presence of hydrogen peroxide, figure 8(b), electrochemical cathodic and anodic response is observed at pH 7.4 only. Prussian blue modified electrode at pH 3, has the highest response of current. GC-MWCNT-PB compared with GC-PB, GC-MWCNT-PB shows good stability of PB film after using different pH solution in the absence or presence of H_2O_2. These results indicate that the presence of MWCNT in the MWCNT/PB composite film significantly enhances the electrochemical stability of Prussian blue nanoparticles. The extraordinary stability of the MWCNT/PB hybrid composite film could be due to the π-π* stacking interaction between carbon atoms in the carbon nanotubes and the –CN groups of PB. Besides, cations in the PB (iron ions) can also interact with anions in carbon nanotubes (carboxyl moieties) through ionic interaction. These results have been reported with PB/MWCNT and OMC/PB composite films that showed the electrochemical and electroanalytical properties of PB were improved in the presence of OMC/PB electrode [33-34].

4. CONCLUSION

In summary, the results presented here demonstrate the use of GC-PB, GC-MWCNT-PB composite for the electrochemical measurement of hydrogen peroxide. Prussian blue is easily synthesized and characterized. Electroanalytical responses and stability were improved when GC-PB and GC-MWCNT-PB modified electrodes were used. Electrochemical responses depended significantly on pH. This shows that the GC-PB and GC-MWCNT-PB modified electrodes will have a significant electroanalytical efficiency in the future. GC-MWCNT-PB and GC-PB electrodes are easily constructed, it responds rapidly and it has a good selectivity.

ACKNOWLEDGMENTS
This work was supported by a research grant from the faculty of applied and computer science research and publications committee of Vaal University of Technology, Vanderbijlpark.

References

1. C. Wang, L. Zhang, Z. Guo, J. Xu, H. Wang, H. Shi, K. Zhai, X. Zhuo, *J. Electroanalysis*. 22(16) (2010) 1867-1872.
2. B. Fang, Y. Feng, G. Wang, C. Zhang, A. Gu, M. Liu, *Microchimacta*. 173 (2011) 27-32.
3. D.J. Yang, C.Y. Hsu, C.L. Lin, P.Y. Chen, C.W. Hu, R. Vittal, K.C. Ho, *Energy Mater. Solar cells*. 99 (2012) 129-134.
4. Z. Li, J. Chen, W. Li, K. Chen, L. Nie, S. Yao, *J. Electroanal. Chem*. 603 (2007) 59-66.
5. B. Haghighi, H. Hamidi, L. Gorton, *Sens. Actuators*. *B* 147 (2010) 270-276.
6. J. Zhang, J. Li; F. Yang, B. Zhang, X. Yang, *Sens. Actuators*. *B* 143 (2009) 373-380.
7. V.D. Neff, *J. Electrochem. Soc.* 125 (1978) 886-887.
8. F. Ricci, G. Palleshci, *J. Biosens. Bioelectron*. 21 (2005) 389-407.
9. P. Salazar, M. Martin, R. Roche, R.D. O'Neill, J.L. Gonzalez-Mora, *J. Electrochima. Acta.* (2010) 6476-6484.
10. F. Ricci, A. Amine, G. Palleschi, D. Moscone, *J. Biosens. Bioelectron.* 18 (2003) 165-174.
11. L. Lin, X. Huang, L. Wang, A. Tang, *Solid. State. Science*. 12 (2010) 1764-1769.
12. N.B. Li, J.H. Park, K. Park, S.J. Kwon, H. Shin, J. Kwak, *J. Biosens. Bioelectron*. 23 (2008) 1519-1526.
13. A.S. Adekunle, B.B. Mamba, B.O. Agboola, K.I. Ozoemena, *Int. J. Electrochem. Sci*. 6 (2011**)** 4388-4403.
14. S. Xing, H. Xu, G. Shi, J. Chen, L. Zeng, L. Jin, *J. Electroanalysis*. 21(15) (2009) 1678-1684.
15. M. Shokouhimehr, E.S. Soehnlen, A. Khitrin, S. Basu, S.D. Huang, *J. Inorg. Chem. Commun.* 13 (2010) 58-61.
16. A.A. Karyakin, *J. Electroanalysis*. 13(10) (2001) 813- 819.
17. Y. Miao, J. Chen, X. Wu, *J. Colliod* 69(3). (2007) 334-337.
18. B. Haghighi, S. Varma, F.M. Alizadehsh, Y. Yigzaw, L. Gorton, *Talanta*. 64 (2004) 3-12.
19. S. Iijima, *Nature*. 354 (1991**)** 56-58.
20. W. Yue-Rong, H. Ping, L. Qiong-Lin, L. Guo-An, W. Yi-Ming, *Chin. J. Anal. Chem.* 36(8) (2008) 1011-1016.
21. D.S. Bag, R. Dubey, N. Zhang, J. Xie, V.K. Varadan, D. Lal, G.N. Mathur, *Smart. Mater. Struct*. 13 (2004) 1263-1267.
22. M. Valcarcel, B.M. Simonet, S. Cardenas, B. Zuarez, *J. Anal. bioanal. Chem*. 382 (2005) 1783-1790.
23. A.S. Adekunle, B.O. Agloola, J. Pillay, K.I. Ozoemena, *Sens. Actuartor*. *B* 148 (2010) 93-112.
24. J. Wang, *J. Electroanalysis*. 17(1) (2005) 7-14.
25. N. Zhang, G. Wang, A. Gu, Y. Feng, B. Fang, *Mirochim. Acta*. 168 (2010) 129-134.
26. A.J. Saleh Ahammad, J.J. Lee, M. Aminur Rahman, *Sensors*. 9 (2009) 2289-2319.
27. Y. Zhang, X. Sun, L. Zhu, H. Shen, N. Jia, *J. Electrochimica. Acta.* 56 (2011) 1239-1245.
28. J. Ping, J. Wu, K. Fan, Y. Ying, *J. Food Chem*., 126 (2011) 2005-2009.
29. M.S. Lin, B.I. Jan, *J. Electrocanalysis* 9 (1997) 340-344
30. S. Ndwandwe, P. Tshibangu, E.D. Dikio, *Int. J. Electrochem. Sci*. 6 (2011) 749-760.
31. A. Gotoh, H. Uchida, M. Ishizaki, T. Satoh, S. Kage, S. Okamoto, M. Ohta, M. Sakamoto, T. Kawamoto, H. Tanaka, M. Tokumoto, S. Hara, H. Shiozaki, M. Yamada, M. Miyake, M. Kurihara, *J. Nanotechnology*. 18 (2007) 345-609
32. S. Han, Y. Chen, R. Pang, P. Wan, *Ind. Eng. Chem. Res.* 46 (2007) 6847-6851.

33. J. Bai, B. Qi, J.C. Ndamanisha, L.P. Guo, *Micropor. Mesopor. Mater*. 119 (2009) 193-199.
34. J. Zhang, J.K. Lee, Y. Wu, R.W. Murry, *Nano. Lett.* 3 (2003) 403-411.